Magnetic properties and spin disorder in nanocrystalline materials

1999 J. Phys.: Condens. Matter 11 9455

(http://iopscience.iop.org/0953-8984/11/48/308)

J. Phys.: Condens. Matter **11** (1999) 9455–9482. Printed in the UK PII: S0953-8984(99)04691-3

Magnetic properties and spin disorder in nanocrystalline materials

A Hernando

Instituto de Magnetismo Aplicado, Universidad Complutense, RENFE, CSIC and Departamento Física de Materiales, Universidad Complutense, PO Box 155 Las Rozas, Madrid 28230, Spain

Received 1 June 1999

Abstract. The more interesting features in magnetism of systems of nanoparticles are reviewed. Tailoring of soft and hard magnetic materials as well as basic studies on magnetic interactions are discussed. Particular emphasis is given to the magnetic properties of the particle shell and grain boundaries, generally different to these of the core, and responsible for phenomena such as interphase exchange penetration, Curie temperature enhancement and magnetic coupling. The magnetic behaviour of different nanocrystalline systems has been described. Spin disorder has been found to be a general trend for the magnetic ground state of the outer shell of magnetic particles. Disorder at the surface can be due to competing interactions with different signs originating from broken bonds or topological disorder (grain boundaries), random surface anisotropy, surface magnetostriction, compositional gradients and in general to the enhanced gradient of different properties at the surface. The spin-glass-like ground state of the surface only affects the macroscopic properties in nanocrystalline samples for which the ratio between the number of atoms at the interface and the number of atoms in the core can be enormous, actually as large as 30%.

1. Introduction and definitions

A polycrystalline sample with grain size of the order of nanometres is called nanocrystalline and forms a particular type of nanostructure. Nanocrystals are generally interconnected by either the grain boundaries or a different matrix. The more relevant aspect of the nanocrystalline samples is the high value of the ratio, N_s/N_v, between the atoms at the interface, N_s, and the total number of atoms, N_v. If we call D the average grain size and a the inter-atomic distance, N_s/N_v varies roughly as a/D, which in the case of grains of nanometric dimensions becomes sometimes as high as 30%. Since the physical environment and thereby the physical properties of the atoms at the interface are different from those of atoms located inside the crystallites, the macroscopic properties are expected to be remarkably affected by the grain refinement. This characteristic allows us to tailor the nanocrystals through the control of both grain size and strength of intergranular connectivity.

Let us focus on ferromagnetic nanocrystals. Generally we mean by ferromagnetic nanocrystalline sample any sample composed of ferromagnetic nanocrystals embedded in a matrix. The matrix or intergranular region can be either the boundary of the nanocrystals or a different phase, magnetic or non-magnetic. The relevant aspect of magnetic nanocrystals is related to the coincidence of the grain size scale (nanometres) with the typical or critical magnetic length, such as exchange length or exchange correlation length. Such scale coincidence gives rise to critical macroscopic properties. Nowadays the outstanding magnetic materials used by engineers for applications are nanostructured because the macroscopic average procedure can be easily controlled at this scale.

0953-8984/99/489455+28$30.00

1.1. Random anisotropy and magnetic interactions

One important characteristic of nanocrystalline ferromagnetic samples is the orientation fluctuation of the local magnetization easy axes. The correlation length of the anisotropy axes is typically of the order of D. The second important characteristic is the degree of coupling, exchange or magnetostatic, between adjacent crystallites carried out through the atoms of the intergranular region which in general exhibit different magnetic properties from the atoms placed inside the nanocrystals. The difference between exchange and magnetostatic coupling is remarkable. Exchange is more intense and localized, whereas dipole–dipole interactions are smaller but long ranged. As discussed below in relation to some examples of Curie temperature enhancement the importance of the localized exchange interactions is predominant at the nanoscale. Exchange from ferromagnetic toward paramagnetic metals can penetrate a few interatomic distances decaying exponentially. But its boundary value at the ferromagnetic side reaches effective fields of 1000 T. Exchange interactions also govern the coupling through insulators driving the spin dependence of electronic tunnelling. On the other hand, the stray fields carrying magnetostatic coupling are of the order of a few teslas but extend over the overall crystallite size. Both types of interaction lead to ordered ground states at low temperatures. The ground state is in general difficult to predict since many types of interaction are present, with different signs. The term spin-glass like structure is normally used to describe these spin disordered and frozen ground states.

When the matrix is paramagnetic, or diamagnetic, and its thickness, d, is high enough to avoid exchange transmission between the grains the nanocrystalline sample can be magnetically considered as an assembly of isolated or weakly magnetostatic interactive single domain particles. These systems have been customarily considered attractive as hard magnetic materials, in the low temperature range, and as superparamagnetic systems at higher temperatures. This is the case of Co–Cu [1], Co–Ag or Fe–Cu [2] granular solids, in which metallic conductivity connects electrically both types of grain, whereas ferromagnetism is exclusively located at the weakly coupled ferromagnetic grains. However, when the matrix is also ferromagnetic the grains and the matrix are exchange coupled and the total system behaves in a collective mode exhibiting in general new and outstanding macroscopic properties. To this second class belong the Fe rich soft nanocrystalline [3] materials as well as the hard spring magnets [4].

1.2. Nanostructures and technical magnetism

The importance of the nanostructure on the macroscopic magnetic properties can be pointed out after reviewing briefly the state of art of magnetic materials for industrial applications. As is well known the magnetic applications can be classified into two large groups: (a) magnetic flux multiplication which requires soft magnetic materials with high magnetization and narrow hysteresis loop, i.e. low coercivity, and (b) magnetic storage of either energy (magnets) or information (magnetic recording); both cases require hard magnetic materials with high magnetization and wide hysteresis loop, i.e. high coercivity and remanence. Since the possibility of increasing the magnetization, always required, is restricted by serious limitations [5] the main task of the research in magnetic materials carried out during this century has consisted in spreading over a wider range the available coercivities. If the saturation magnetization $\mu_0 M_s$ of the ferromagnetic alloys is typically of the order of 1 T the coercivity $\mu_0 H_c$ ranges between 10^{-7} T for the softer magnetic material and 5 T for the harder magnets. Therefore, the seven orders of magnitude which separate in coercivity the softer from the harder alloys should be considered as a suitable index of the success of the science of magnetic material.

However what is really remarkable is that the softest material $Fe_{79}Zr_7B_9$ ($\mu_0 H_c = 10^{-7}$ T) as well as the hardest material $Fe_{79}Nd_7B_9$ ($\mu_0 H_c = 1$ T) known in 1999 are obtained from amorphous alloys with closely related compositions. Notice that only a difference of 7 at.% in content gives rise to a difference of seven orders of magnitude in coercivity. The reason for such an enormous difference is the nanostructure obtained by partial devitrification of the initial amorphous state. Both types of sample consist of a soup of nanograins embedded in a softer matrix. In partially crystallized $Fe_{79}Zr_7B_9$ Fe nanocrystals with anisotropy constant, k_1, of the order of 10^4 J m^{-3} are embedded in the magnetically softer residual amorphous matrix, whose composition depends on the crystallized fraction x, whereas in devitrified $Fe_{79}Nd_7B_9$ hard nanocrystals of the $Nd_2Fe_{14}B$ phase, with anisotropy constant $k_1 = 10^7$ J m^{-3}, are dispersed in a softer matrix formed by nanocrystalline Fe. If is assumed that the coercivity term depending on k can be expressed as

$$H_c = \alpha 2k/\mu_0 M_s \tag{1}$$

the expected difference in coercivity between FeZr and FeNd nanostructures should be that of the anisotropy constant: three orders of magnitude. However, the nanostructure of the FeZr sample reduces by itself the effective macroscopic anisotropy by four orders of magnitude, whereas the nanostructure of FeNd alloy enhances the magnetization and the energy product, a factor which describes the energy stored by a magnet.

1.3. Nanometric scale of the characteristic magnetic lengths

The influence of the nanostructure on the average or macroscopic anisotropy of a ferromagnetic or ferrimagnetic solid is a beautiful example of the dependence of properties on the ratio between structural lengths and typical or characteristic magnetic lengths. In a ferromagnetic homogeneous specimen the following characteristic lengths are normally defined [6]:

(1) Exchange length, L_{ex}, measures the particle size below which the magnetostatic energy associated with an uniform magnetization is smaller than the exchange cost required to demagnetize the particle, therefore the material is expected to be a single domain when its size is smaller than L_{ex}. When the particle size is larger than L_{ex} the decomposition in domains becomes energetically favourable. L_{ex} is defined as

$$L_{ex} = (2A/\mu_0 M_s)^{1/2} \tag{2}$$

where A is the exchange constant, typically of the order of 10^{-11} J m^{-1} in 3d ferromagnetic metals. L_{ex} takes the following values: 2.8 nm for Fe, 3.4 nm for Co and 9.9 nm for Ni.

(2) Exchange correlation length or wall thickness, L, is defined as

$$L = (A/k)^{1/2} \tag{3}$$

where k is the anisotropy constant. L measures the distance at which a local fluctuation of the spin alignment propagates through the material. It is therefore the typical thickness of the domain walls and therefore those particles with size smaller than L, even though they are larger than L_{ex}, cannot have domains. L takes the following values: 18 nm for Fe, 5.5 nm for Co and 51 nm for Ni. It actually determines the size barrier between single and multidomain structures.

It is important to remark that the characteristic lengths defined above are in the range of nanometres. Thus, the magnetic behaviours of the nanocrystals are actually expected to be strongly dependent of the ratio D/L. Even though L_{ex} is almost temperature independent,

the characteristic length, L, depends on temperature and increases as the temperature does. Therefore, particles in the size range of nanometres should exhibit peculiar and anomalous thermal dependence due to the change induced by temperature in the ratio D/L. The coercive field is closely related to the exchange correlation length. Short L is, with great generality, related to high coercivity and vice versa. In a single magnetic phase coercivity always decreases with temperature, whereas L monotonically increases. Notice that anisotropy falls down with temperature faster than the magnetization does and therefore, according to (1), H_c decreases with temperature. As will be shown below the increase of coercivity with increasing temperature often becomes a hint of nanoscale mixing of heterogeneous phases.

1.4. Average procedure for the macroscopic properties in nanostructures

The macroscopic or effective anisotropy, k^{eff}, of a nanocrystalline sample depends on (1) the anisotropy and exchange constants, k_1, k_2, A_1 and A_2, of grains and matrix respectively (it will always be considered that $k_1 \gg k_2$, as corresponds to the cases of interest mentioned above of NdFe and ZrFe), (2) the exchange coupling between the grains, A^*, which in general can be written as $\gamma(A_1A_2)^{1/2}$, γ being a factor describing the ability of the interface to transmit exchange, (3) the grain size, D, through the ratio $D/(A^*/k_1)^{1/2}$ and (4) the intergranular distance or matrix thickness, d, through the ratio $d/(A^*/k_2)^{1/2}$.

Let us suppose that $(A^*/k_2)^{1/2} = L_2^*$ is larger than d; in this case any grain is informed of the presence of the other grains. If it is also true that $(A^*/k_1)^{1/2} = L_1^* > D$ the grains should be not only informed but coupled by exchange interactions. In other words if it is simultaneously verified that $L_2^* > d$ and $L_1^* > D$ the matrix induces a softening of the grains. When $L_2^* > d$ but $L_1^* < D$, the matrix is coupled to the grains, which remain uncoupled themselves, and therefore the matrix undergoes an effect of hardening induced by the presence of the grains. Finally, if $L_2^* < d$ and $L_1^* < D$ the system is weakly coupled and the magnetic behaviour tends to be that of the average of both phases separated. In this last case a light deviation from the pure average is introduced by the weak coupling which decreases in strength as L_2^*/d and L_1^*/D decreases toward zero.

An interesting problem in heterogeneous magnetic systems, such as polycrystalline, nanocrystalline or amorphous samples, is to find the correct procedure to obtain the weighted average anisotropy. The correct procedure strongly depends on the degree of magnetic coupling. A simple, but illuminating picture of the smoothing effect of the nanostructure on the effective anisotropy when $L_2^* > d$ and $L_1^* > D$ are simultaneously verified is to consider only the single phase formed by crystallites, neglecting the matrix. Then, $A^* = \gamma A_1$ and $L_1^* = (\gamma A_1/k_1)^{1/2}$ which is assumed to verify $L_1^* \gg D$. The exchange A^* tends to align the magnetic moments of the different grains parallel to each other. However the anisotropy tends to align the magnetic moment at each grain along the local axis. Since the local axis orientation fluctuates from grain to grain there is a compromise between exchange and anisotropy. The two limiting cases of such compromise correspond to: (a) when the anisotropy is much stronger than the exchange ($L_1^* \ll D$) each magnetic moment lies close to the local axis and the magnetic order is frustrated, (b) the opposite case, if the exchange is stronger than the anisotropy ($L_1^* \gg D$) the magnetic moment are aligned even though in this configuration a cost of anisotropy energy arises. If the easy axes are randomly distributed in orientation and the number of different easy axes (or number of grains) contained in the region in which the magnetic moments are exchange coupled is N, the effective anisotropy, as nicely shown by Alben *et al* [7] using random walk considerations, falls down to $k_1/(N)^{1/2}$.

1.5. Outline of this article

The study of the magnetic properties of isolated fine particles has been traditionally urged by both a technological and theoretical interest connected with the possibility of developing a better understanding of magnetic phenomena related to size effects. From the technological perspective the interest of fine particles is associated nowadays with magnetic memory in view of their potential applications in high energy magnetic recording as well as with the technical possibilities derived from magnetic ferrofluids. Many years ago fine particle production was an interesting target in order to obtain single domain structures with suitable characteristics for magnets. From the theoretical point of view three important basic research fields have been traditionally linked to nanosized constituent particles or crystallites: (i) magnetization reversal, coherent or incoherent modes and micromagnetic calculations, (ii) magnetic relaxation by different modes such as, recently, quantum tunnelling, superparamagnetic behaviour and magnetic interactions and (iii) surface magnetism associated with the large surface/volume ratios.

Many books and articles [8] have outlined the more interesting aspects of the magnetic relaxation and magnetization reversal in systems formed by nanometric particles obtained by different physical and chemical methods. In particular superparamagnetism in systems of interactive particles has been thoroughly described. The effect of interactions at low temperatures can give rise to collective magnetization modes which are also discussed in detail. Morup and his group [9] have performed an extensive Mössbauer analysis in order to analyse the dependence of the blocking temperature on the interactions. They found a decrease of the relaxation time with the enhancement of interactions. Such result is in disagreement with theoretical predictions derived from models by Shtrikman and Wohlfarth [10] and by Dormann *et al* [11]. Thus, the correlation between relaxation time and magnetic interactions is an open question which drives a huge number of discussions in regular conferences on nanoparticles. The interest of this subject has been recently enhanced with the proposal of macroscopic quantum tunnelling as a new relaxation mechanism observable at very low temperatures. Chudnovsky and Tejada [12] have also written an interesting book, *Quantum Tunneling of the Magnetic Moment*.

In this article the outstanding characteristics of the nanocrystalline magnetism are described in the following order. First, the magnetic properties of the grain boundaries in a single phase system, as is the case of pure nanocrystalline Fe, are reviewed. Mössbauer spectroscopy is used as a useful tool capable of recognizing the boundary magnetic contribution. Second, the magnetic characteristics of the surface of magnetically isolated iron oxide nanoparticles and magnetically connected FeRh nanocrystals are described. The main focus is centred on spin disorder and the magnetic coupling between the surface atoms and the atoms located inside the particle. Third, the magnetic behaviour of a granular solid formed by non-miscible elements, such as FeCu, is described. It is shown that many of the structural configurations obtained during the different steps of the decomposition are often characterized by fluctuations of the local magnetic constants with correlation lengths of a few nanometres. Fourth and finally, the random magnetic anisotropy effect on macroscopic properties in amorphous and nanocrystalline materials is discussed on the basis of some experimental results concerning two-phase systems. The analysis tries to show the capability of tailoring magnetic properties for applications provided by nanostructures.

2. Nanocrystalline Fe: Mössbauer and magnetism of grain boundaries

It is somehow amazing that Fe, that has long been considered the archetype of a ferromagnetic material and has been carefully scrutinized for decades, exhibits *new* and *singular magnetic*

behaviour when it is in the form of nanostructures. In this sense, pure iron nanostructures are perhaps the most fundamental case of the physical processes described above: the appearance of unique magnetic properties due to the different physical behaviour of interface atoms with respect to those in the bulk [13].

By no means are the structures of these nanostructures well characterized at the atomic level. On the one hand, the difficulties related to the structural analysis of amorphous systems, due to their lack of periodicity, are well known. Moreover, a number of unusual crystalline or quasi-crystalline structures emerge at the boundaries between the different nanoparticles and between the nanoparticles and the embedding matrix. Although a number of contemporary techniques (such as Mössbauer spectroscopy) are beginning to throw light on the nature of these new structures, there are still many unanswered questions. It is also worth remarking that, as most of these nanostructures are *far from equilibrium*, the accurate characterization of the preparation processes is mandatory as, otherwise, our understanding of the various processes can be plagued by lack of reproducibility of the results.

Fe is known to present different phases [14]. Under normal conditions, up to about $T_0 = 1183$ K, ferromagnetic bcc Fe (α-Fe) with a magnetic moment per atom of 2.2 μ_B, is the only phase present. Above T_0, an fcc phase (γ-Fe) appears, that remains stable up to 1663 K. It has been theoretically predicted that fcc iron could exist in, at least, two different states: a high moment, high volume state ($\mu = 2.3$–$2.8\ \mu_B$, lattice constant $\geqslant$3.6 Å) and a low moment state ($\mu \leqslant 1.6\ \mu_B$) with a lower lattice constant (between 3.5 and 3.6 Å), the latter having antiferromagnetic ordering with a Néel temperature about 67 K. However, experimental confirmation of these theoretical predictions is difficult because it is hard to maintain metastable fcc structures at low temperatures. As an alternative approach, one can resort to derive indirect evidence from closely related systems, such as Fe epitaxial films grown onto Cu(001), although of course a limit in their thickness is rapidly reached at 2–3 atomic layers.

An antiferromagnetic low moment (around 0.7 μ_B) state—denoted γ_1—with a Néel temperature of about 67 K has been identified in small fcc Fe precipitates in supersaturated Fe–Cu alloys, as is discussed in section 4 of this article.

Intriguingly enough, an Fe phase rather similar to the one detected in the Fe–Cu system has been also detected in nanostructures of pure Fe. Whereas in the former case relatively minor Fe volumes are forced to adopt the fcc structure by external constraints, in the case of pure Fe this magnetically ordered fcc phase forms at the interface between bcc crystals, following thermally induced rearrangement of the grain boundary region. Evidence of the nature of that phase has been obtained by joint Mössbauer, magnetization and transmission electron microscopy (TEM) analysis of pure ball-milled Fe for different milling times and after subsequent thermal annealings [14]. It is worth pointing out that after 1 hour annealing at 920 K both structural and magnetic properties of the original bulk polycrystalline Fe are re-obtained. This also denotes that introduction of impurities during the milling and annealing processes is kept at a minimum.

The new phase is identified mainly on the basis of its Mössbauer spectrum. Figures 1(a), (b), (c) show, for comparison, the Mössbauer spectra of the sample after milling (limiting state) and after annealing at two increasing temperatures. One can see that the magnetic hyperfine field (HFF) distribution profile changes dramatically. After the thermal treatment at 570 K (figure 1(b)), a narrow peak centred on 21 T becomes visible. With increasing annealing temperature, its relative weight increases at the expense of the original contributions at higher fields (figure 1(c)). The values of the relative resonant area linked to the HFF distribution are also reported in the caption of figure 1. These data strongly suggest that a rearrangement of the atoms at the interface occurs mainly in the 570–670 K temperature range. As a Mössbauer sextet spectrum is characteristic of a magnetically ordered configuration, the appearance of the

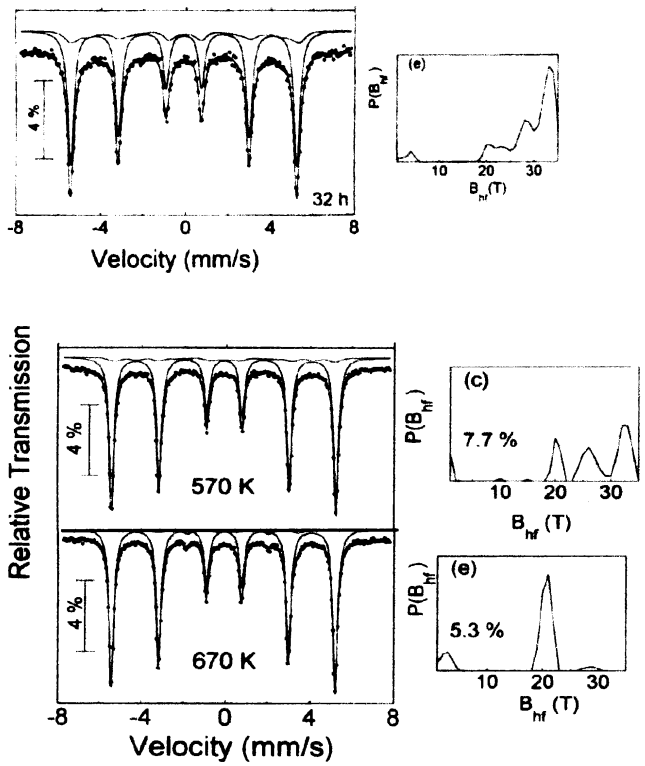

Figure 1. Room temperature Mössbauer spectra (left-hand side) and relative hyperfine magnetic field distributions (right-hand side) corresponding to as-milled Fe and to milled powders subsequently subjected to 1 h thermal treatments at the indicated temperature. Percentages of Fe atoms at the boundaries obtained from the resonant area linked to the hyperfine field distribution are 8.5%, 7.7% and 5.3% for 1(a), (b) and (c) respectively.

peak at 21 T in the HFF distribution indicates that, during grain boundary thermal relaxation, not only does the bcc configuration recover, but also a magnetically ordered Fe phase, unlike the usual α-phase, is formed.

The 21 T hyperfine component of the spectrum has been interpreted as arising from regions of a ferromagnetic fcc Fe structure (γ_2-Fe). This is done, first, on the grounds of their Mössbauer spectra, that are quite similar to the ones observed in the γ_2 phase of Fe in Fe–Cu samples (see section 4). The existence of an fcc phase is supported by TEM analysis. On annealed samples, along with the spots corresponding to the usual Fe bcc phase one can find another set of spots corresponding to a slightly smaller nearest neighbour parameter. In figure 2 one can observe both the spots corresponding to a 'normal' bcc crystallite close to the (111) orientation and the encircled spots, identified as a fcc structure of lattice parameter 3.51 ± 0.05 Å, close to the (211) orientation. It is worth remarking that both bcc and fcc structures are coherent with an orientational relationship of $[110]_{bcc} \circ [111]_{fcc}$. A straightforward geometrical analysis reveals that this relationship implies that the two most densely packed planes of the two structures—$(110)_{bcc}$ and $(111)_{fcc}$—superimpose on each other, which agrees with the rule governing most epitaxial systems of bcc materials grown on fcc substrates. This mutually oriented structure probably results from grain boundary rearrangements which occur in the 570–670 K temperature range.

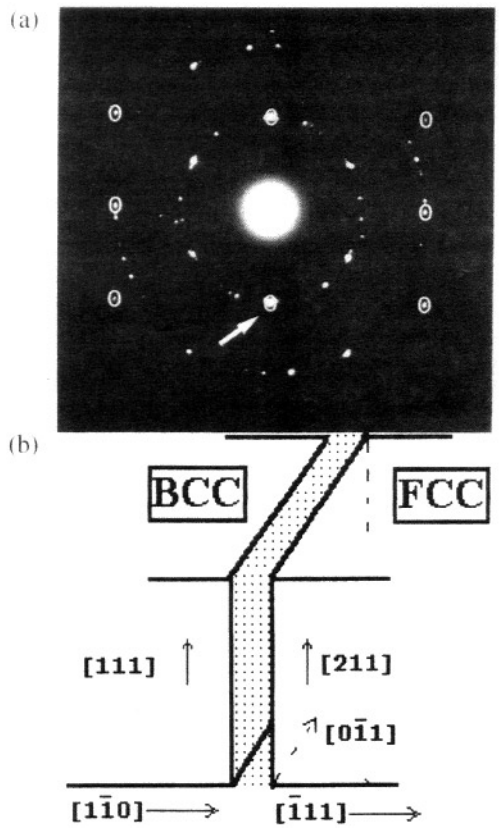

Figure 2. (a) SAD pattern of the annealed sample. The rings correspond to the Fe bcc phase close to the [111] zone axis orientation; the encircled spots can be indexed in terms of the [211] zone axis electron diffraction pattern of an fcc structure of lattice parameter 3.51 ± 0.05 Å. The arrow points to the superposition of $(110)_{bcc} \parallel (111)_{fcc}$ reflections. (b) Direct lattice construction associated with the geometry of (a). The shaded area corresponds to the plane of growth. The spreading of the distribution around 33 T suggests that, for a number of atoms at the interface, the surrounding environment is not greatly different from that of bcc bulk iron, probably due to a closer location to the core of the nanocrystals. The contribution observed at 26 T can be explained by a reduction of the coordination number [11], a wide distribution of nearest neighbour distances at the grain boundary together and/or a reduction of short range order [12], although the experiments reported here do not allow a definite elucidation of the controlling mechanism.

Magnetic measurements confirm the Mössbauer indication that the new phase is ferromagnetic. By measuring the evolution of the magnetization at $T = 560$ K, as illustrated in figure 3, after 20 hours annealing, M has decreased by about 13%, with respect to its value at the very beginning of the measurement. Once the sample is cooled down again to room temperature, the magnetization of the sample—at $H = 10$ kOe—is about 3% lower than before the annealing. When a magnetization measurement is performed in a further isochronal annealing of the same sample, a decrease of M is clearly observed at ∼500 K. This can be explained in terms of a magnetic order–disorder transition of the new phase that is formed during the isothermal measurement and which, therefore, is interpreted as *ferromagnetic*. Accordingly, the considerable reduction of M—about 13%—in figure 3 can be explained assuming that the isothermal measurement has been carried out at a temperature higher than

the Curie temperature of the new phase that is being formed in the course of the measurement. The reduced magnetization value (figure 3, inset), measured at room temperature, after the prolonged annealing at 560 K, indicates that the magnetic moment for Fe atom in the fcc configuration is lower than in the as-milled state.

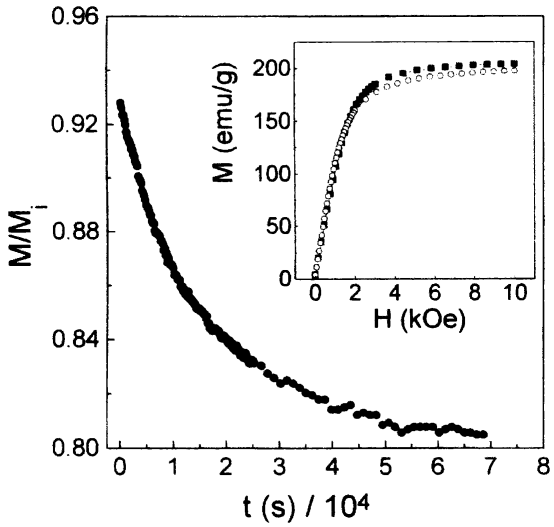

Figure 3. Time dependence of the magnetization (M) at $T = 560$ K of nanocrystalline Fe (applied field $H = 10$ kOe). M_i is the room temperature magnetization value of the as-milled sample. In the inset: room temperature M as a function of the applied magnetic field H for the nanocrystalline sample before (full squares) and after (open circles) the isothermal measurement.

Both the Fe–Cu and the pure Fe data show that rather unusual atomic arrangements are found near the boundaries of the individual particles in nanostructures. These boundaries seem to stabilize—even at room temperature—structures with a coordination number different from the bulk, and, consequently, singular values of the average magnetic moment per atom. Apart from its intrinsic interest in terms of fundamental physics, understanding these nanostructures might well be an effective way to control specific magnetic properties.

3. Spin disorder at the surface of magnetic nanoparticles

In recent years many experimental observations have pointed out the anomalous magnetic behaviour of the atoms located at the particle surface compared with that of the inner atoms. The experimental results have shown that there exist different degrees of coupling between inner and surface atoms and that the surface spin structure is different to the inner particle magnetic structure.

An important property of many fine magnetic oxide particles is the high susceptibility exhibited at high applied fields and the difficulty of saturating them even under strong magnetic fields, much larger than the possible anisotropy fields. In the region close to saturation the hysteresis loop is open, with positive and negative field sweeps well separated. A number of articles have been published during the last few years dealing with the magnetic behaviour of Fe, Co and Ni nanocrystalline particles, mainly prepared by the inert gas condensation method, and presenting different degrees of surface oxidation [15–20]. More recently the

magnetic characteristics of particles with compositions NiO, $NiFe_2O_4$ and γ-Fe_2O_3 have been thoroughly studied by the group of Berkowitz [21, 22]. These oxides, as well as oxygen passivated Fe, Ni or Co nanoparticles, exhibit, apart from the low magnetization and high susceptibility at high fields, shifted hysteresis loops after field cooling. Both characteristics disappear above a critical temperature T_B. Since $NiFe_2O_4$ particles are not saturated even under fields of 160 kOe which is 400 times stronger than the anisotropy field there must be a cause different from the anisotropy responsible for the lack of saturation [23]. From field cooling, FC, and zero-field cooling, ZFC, magnetization measurements at very high fields it is obvious that below T_B the magnetization is at a non-equilibrium state for the ZFC case. The presence of a high field irreversibility is also obvious from the strength of the fields, 70 kOe, in which the separation between FC and ZFC curves still remains. Notice the enormous quantitative difference with the typical separation between ZFC and FC curves for spin glasses, which is normally obtained in fields lower than 100 Oe. In oxygen passivated γ-Fe_2O_3 and Fe nanoparticles the difference between ZFC and FC curves has been also observed in fields of 50 kOe [24].

With the help of relaxation measurements, Berkowitz's group [22, 23] has explained the general magnetic behaviour described above as a consequence of the magnetic structure of the surface atoms. In the case of ferrimagnetic and antiferromagnetic oxides the magnetic coupling is carried out through superexchange interactions that are very sensitive to the atomic environment. Because of the broken symmetry at the surface, broken bonds and some degree of structural disorder, the exchange interactions fluctuate in both strength and sign and thus the magnetic structure of the surface atoms should correspond to a spin-glass-like configuration or to a spin disordered system. Actually, the existence of many surface spin states separated by energy barriers which could be overcome by the thermal energy would explain the shifted hysteresis loops. Calculations performed by Kodama *et al* [23] have shown the expected energy barrier to be in the range of 50 mK which is well below the freezing temperature, T_B, always ranging between 30 and 60 K. Therefore, they claimed that surface atoms can have a large crystal field splitting due to the asymmetry of the local structural configuration.

The spin disordered state at the particle surface accounts for more of the intriguing characteristics of the magnetic behaviour of nanoparticles at low temperatures. Spin canting in these types of sample had been observed before and the occurrence of a transition to a spin glass state at low temperature had been invoked from observations of magnetic hyperfine splitting. The influence of the surface morphology on the coercivity of nanoparticles with the same size was carefully studied by Hadjipanayis and coworkers [25] who found a clear separation between core and shell magnetic behaviour. From measurements performed on particles of the same size and composition, but with different coatings and different oxidation degrees, it turned out that the intensity of coupling between core and shell is very sensitive to the surface morphology. Particles with different coatings exhibit different thermal dependence of coercivity and different saturating fields. The influence of the surface and interface anisotropy has also been invoked as the origin of the anomalous magnetic properties of nanoparticles at low temperature. In fact, anisotropy also fluctuates at the particle surface and can reach higher values than those of the core. For instance, magnetoelastic coupling developed by surface–core stresses and enhanced by large surface magnetostriction values [26] can also contribute to the surface anisotropy which through the exchange coupling can remarkably modify the magnetization curve of the core.

Recent measurements in FeRh nanocrystalline samples obtained by ball milling have shown a similar behaviour to that exhibited by oxides and oxide passivated nanoparticles at low temperature [27]. The grain size ranged between 7 and 17 nm. The ac susceptibility

(figure 4) and the FC and ZFC magnetization curves obtained under applied fields of 5 kOe are separated below 60 K temperature for which the ZFC curve shows a maximum (figure 5). It is important to remark that this maximum does not appear in the bulk sample and therefore it seems actually to be a consequence of the nanocrystallization process. A careful experimental analysis carried out by using Mössbauer spectroscopy, magnetization and ac susceptibility measurements has pointed out that the overall behaviour can be explained as a consequence of the spin disorder at the grain boundaries. The hysteresis shift observed after FC, illustrated in figure 6, and both the open hysteresis loop and high susceptibility at high fields indicate a similar behaviour to that observed in nanoparticles of magnetic oxides and also suggest a similar origin.

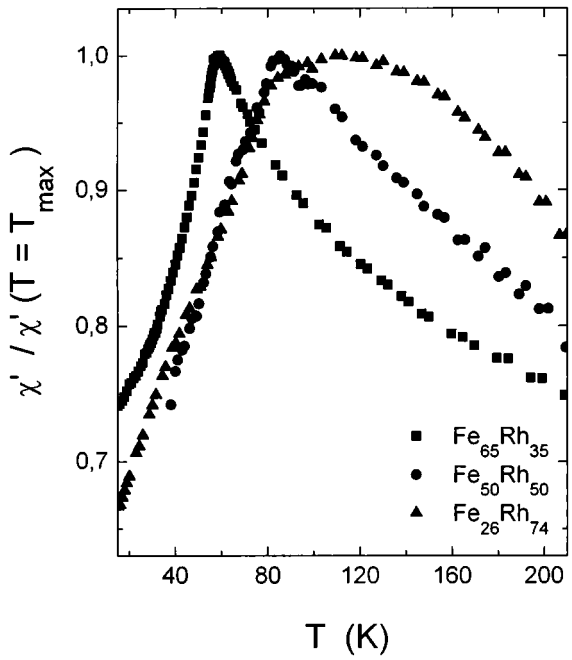

Figure 4. Real part of the ac susceptibility as a function of temperature of FeRh powders measured in a dc field of 100 A m^{-1} and frequency of 111 Hz. The values are normalized by the susceptibility at $T = T_{max}$.

As is known, bulk FeRh equiatomic alloy, with CsCl-like ordered crystalline structure, undergoes a structural transformation close to room temperature from an antiferromagnetic to a ferromagnetic spin structure. Remarkable changes in electrical conductivity [28], entropy [29] and unit cell volume [30] take place during the transformation [31]. In particular the lattice constant of the antiferromagnetic low temperature phase is 2.987 Å. whereas it rises up to 2.997 Å in the ferromagnetic state. Consequently it becomes evident that ferromagnetic and antiferromagnetic interactions coexist in the FeRh system with a relative strength which depends on the interatomic distances. The nanocrystallization procedure (ball milling) drives the powders from the bcc ordered to a fcc disordered structure with non-compensated antiferromagnetic order. The interatomic distance fluctuation at the grain boundary, strongly deformed after milling, gives rise to spin disordered configurations.

It can be concluded that spin disorder at the interfaces is a magnetic structure not only linked to broken bonds in oxides in which spin coupling is due to superexchange interactions. Metallic

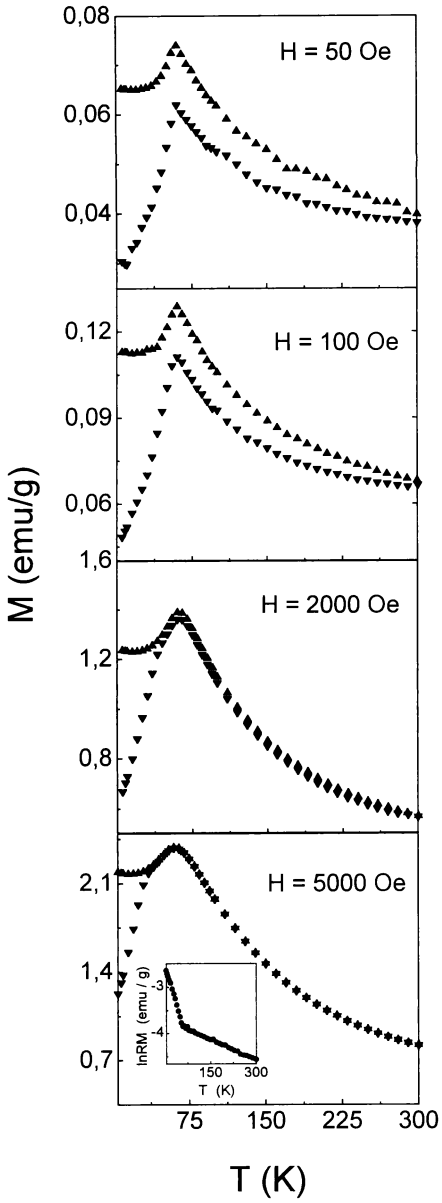

Figure 5. Magnetization against temperature for different fields of ball-milled $Fe_{65}Rh_{35}$ measured during heating after zero-field cooling (ZFC, ▼) and field cooling (FC, ▲). Inset: remanent magnetization (after cooling down in a field of 100 Oe), as a function of temperature for $Fe_{65}Rh_{35}$.

systems with competing interactions of opposite sign can also eventually exhibit spin disorder at the grain boundaries. Random surface anisotropy with high local anisotropy constants would also break down the magnetic order associated with ferromagnetism or antiferromagnetism and generate spin disorder similar to that characteristic of asperomagnetic structures in amorphous materials with strong non-symmetric crystal or local electric fields.

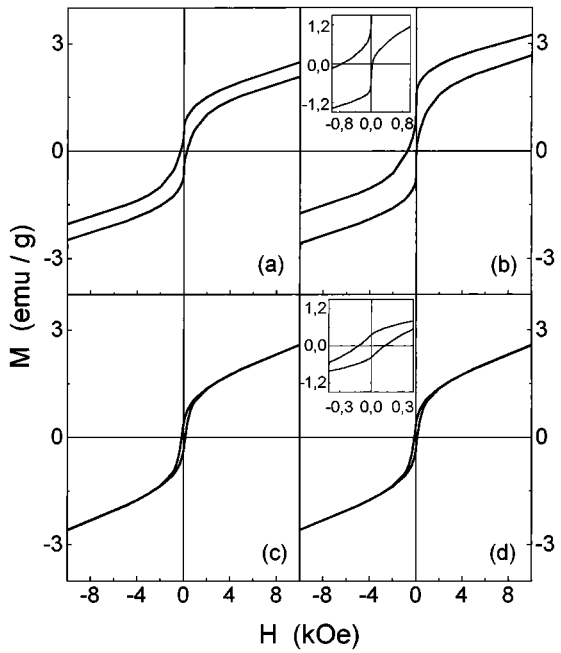

Figure 6. Hysteresis loops for $Fe_{50}Rh_{50}$ at $T = 5$ K (a) after zero-field cooling and (b) after field cooling in a field of 2 T, and at $T = 100$ K (c) after zero-field cooling and (d) after field cooling in a field of 2 T.

An important result of the effect of magnetic disorder at the grain boundary on the macroscopic magnetization curve is that the magnetic, ground and excited, states corresponding to the inner core of the particles and to the surface are different and characterized by different relaxation times. The complex relation of both relaxation times gives rise to anomalous macroscopic relaxation behaviour that sometimes has been considered as possibly originated by macroscopic quantum tunnelling [23]. It is necessary to distinguish between the surface structure and the surface–inner core coupling. The coupling between the inner core and the surface turns out to be different for temperatures below the freezing temperature of the surface spin disorder. Above the freezing temperature the relaxation time of the surface structure becomes shorter and the core is weakly or, in general, differently coupled to the surface. Actually, the surface freezing temperature is also affected by the core, but in order to understand with a simpler picture the particle behaviour it is useful to consider the surface as a different magnetic material. In this picture, the nanoparticle is described as a magnetic bilayer with a peculiar spherical symmetry. One should then consider two magnetic media with different anistropies, interactions and magnetic structures. Both different magnetic phases are magnetically connected through an interphase coupling. It has been shown that this coupling affects the intrinsic properties such as order temperature and magnetic moment of the constituents [32–35]. If, instead of magnetically isolated particles, we analyse magnetic nanoparticles embedded in a magnetic or non-magnetic metallic matrix, the picture becomes much more complex. In this case, the bilayer picture changes into a multilayer description. Let us describe an example.

It has recently been shown that the system formed by a 10% volume fraction of Co nanocrystals finely dispersed in a soft residual amorphous phase exhibits a maximum of ac

susceptibility around 200 K which decreases by two orders of magnitude for lower temperatures [36], as shown in figure 7. The system is obtained at the initial states of the partial devitrification of the amorphous alloy $Co_{80}B_{20}$. This result can be explained as follows. At low temperatures the magnetically hard Co nanocrystals are exchange coupled to the residual amorphous phase producing an overall hardening of the system. As the temperature rises some boron rich layers surrounding the Co crystallites reach their Curie temperatures and the matrix loses the magnetic connection to the Co grains. The cut-off of interphase coupling allows the matrix to recover its magnetic softness. In this case the coupling through the interface disappears by the effect of the compositional gradient along the perpendicular direction of the grain surface. Such a perpendicular compositional gradient has been thoroughly analysed in soft nanocrystalline materials mainly by Mössbauer spectroscopy but also by standard calculations [37–39].

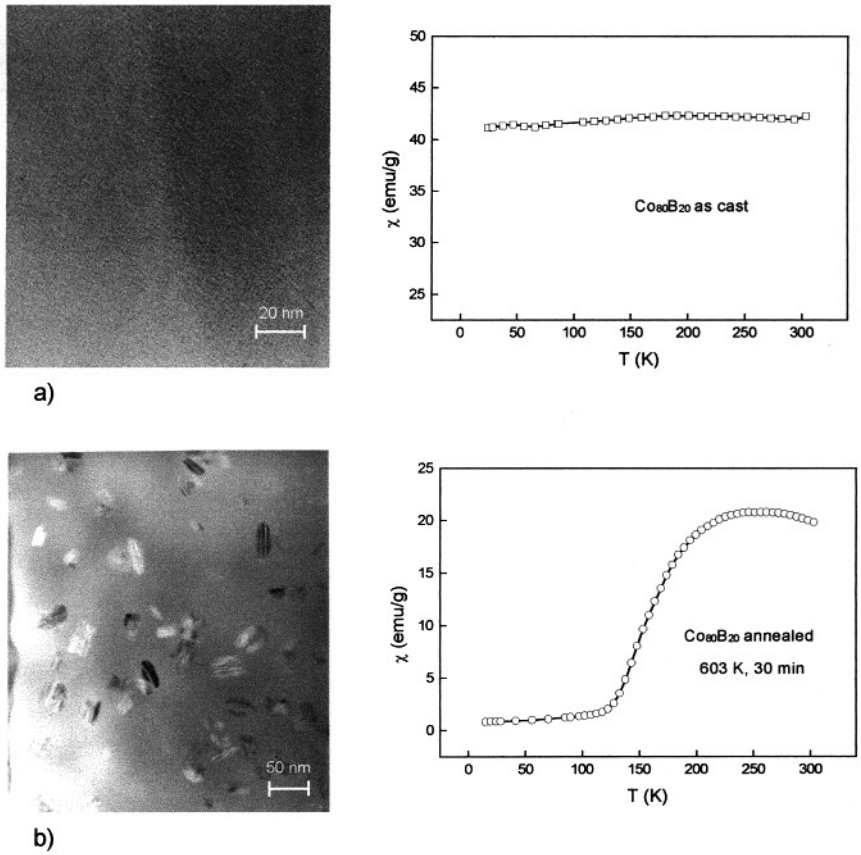

Figure 7. TEM images and temperature dependence of the susceptibility $Co_{80}B_{20}$ melt-spun ribbon in the as-cast state (a) and after annealing at 603 K for 30 minutes (b).

In summary, the grain boundary of nanoparticles can generally be thought of as a magnetic phase different to the inner core. The presence of canting of magnetic moments detected by Mössbauer [40], high susceptibility at high fields, extremely high saturating fields, hysteresis shift after FC, irreversible processes detected by comparing FC and ZFC curves at high fields and a remarkable decrease of the ac susceptibility at low temperatures well below the divergence

point of FC and ZFC form the main experimental features. These magnetic properties point out both the presence of spin disorder at the surface, frozen in below a freezing temperature, and its effect through the surface-inner core coupling on the magnetization curve of the overall system below the freezing temperature. It is to be emphasized that, as has been shown above, many different causes can contribute to the surface spin disorder of nanoparticles. The gradient of different properties through the interface is in fact the origin of the surface magnetic peculiarities. Broken bonds, broken symmetry, topological disorder, high density of defects as dislocations, high surface magnetostriction, strong random anisotropy, coating or compositional gradients at the surface lead in general to splitting of the particle into two magnetic phases: shell and inner core.

4. Metastable nanocrystalline immiscible alloys and granular solids

The development of non-equilibrium processing methods has allowed the formation of immiscible alloys with high enthalpy of mixing. Metastable alloys have been synthesized by vapour quenching, sputtering, ion beam mixing, rapid quenching and ball-milling. After heating, the immiscible two-component alloys such as CoFe or FeCu decompose into a nanocrystalline structure formed by nanocrystals of the constituents and generally known as granular structure. Since the ferromagnetic grains are single domains, the whole system is ideal for study of rotation magnetization processes and magnetic interactions between the particles. At the different steps of the decomposition process, new and interesting structures such as those associated with spinoidal-like decomposition are often observed.

4.1. Granular solids as GMR samples

In 1992 Xiao *et al* [1] and Berkowitz *et al* [1] simultaneously reported giant magetoresistance, GMR, results obtained in the granular CoCu system. With this observation, it was concluded that the origin of the GMR is related to the change of the spin orientation in distances shorter than the mean free path of the electrons. In granular solids composed of magnetic and non-magnetic nanocrystallites, the spatial fluctuation of the spin orientation is a consequence of the random orientation of the crystallites and therefore of their easy axes of magnetization. On the other hand, the spin orientation fluctuation in magnetic, non-magnetic, multilayers, in which GMR was discovered in 1988, is due to the antiferromagnetic coupling between adjacent ferromagnetic layers [41]. Now is generally accepted that, independently of the cause, the random change in spin orientation in short distances is the origin of the GMR. Since the production method of granular solids is easier and less expensive than those methods used to obtain the more perfect multilayers, many research groups made an effort to obtain by different methods granular solids with GMR behaviour. Another cause of the promising perspectives of granular solids is the capability of being tailored at nanostructural scale by suitable annealing treatments. The melt-spinning method allows large quantities of bulk granular materials to be obtained in the form of ribbons. The groups of Allia at Torino and Madurga at Pamplona [42] have reported an interesting set of articles in which the GMR and the magnetic behaviour of Cu_{100-x}–Co_x granular alloys obtained by rapid quenching have been carefully analysed. As is characteristic in most of the nanoparticle systems, the interactions between magnetic particles as well as the grain size distribution must be taken into account in the theoretical framework to explain the experimental results.

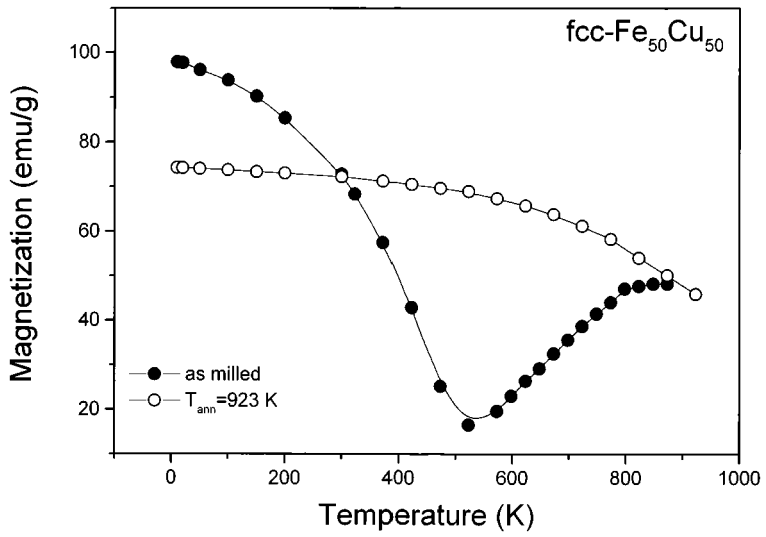

Figure 8. Low and high temperature magnetization measurements of as-milled fcc $Fe_{50}Cu_{50}$ alloy (●) and after the precipitation of bcc Fe (○) showing the crossover at room temperature and the lower magnetic moment.

4.2. Magnetism of nanocrystalline metastable FeCu solid solutions

As an example of the increasing interest developed during the last decade in the magnetic properties of immiscible alloys let us summarize briefly the more interesting results related to Fe–Cu alloys obtained by ball milling. The production and subsequent magnetic characterization of supersaturated Fe–Cu alloys have attracted great interest from the point of view of fundamental research. Supersaturated solid solutions of Fe–Cu were obtained by Sumiyama *et al* [43]. using rf sputtering, further extending the miscibility of Cu in bcc Fe up to 60 at.% and Fe in fcc Cu to nearly 40 at.%. Chien *et al* [44] reported the magnetic and structural properties of a wide range of Fe_xCu_{100-x} alloys prepared via magnetron sputtering. Since 1983, Jilman and Benjamin [45], Uenishi *et al* [46], Ma *et al* [47] Eckert *et al* [48, 49] and Yavari *et al* [50] have reported the production of nanocrystalline Fe_xCu_{100-x} alloys by mechanical alloying. Fe–Cu alloys are ferromagnetic at room temperature over almost all the compositional range. For $x < 60$ the alloys are fcc with a lattice parameter which increases with milling time. For $x > 60$ the structure becomes bcc. Harris *et al* [51] using EXAFS provided structural evidence that both the Fe and Cu atoms reside in an fcc lattice in $Fe_{30}Cu_{70}$ and $Fe_{50}Cu_{50}$ ball milled alloys. The results showed that the near neighbour chemistry is very close to the normal stoichiometry of the starting materials, thus confirming the mixing at an atomic level. By modelling the EXAFS data, the atomic radii of both elements were deduced. According to this model a clear dilation between unlike atoms pairs was pointed out. This model accounts for the lattice expansion observed by x-rays by many authors. The observation of ferromagnetism in fcc Fe–Cu alloys is an intriguing feature since fcc Fe and fcc Cu are not ferromagnetic in their ground state. The calculation of the Fe magnetic moment in different alloys is generally a difficult task. Such difficulty has been often attributed to the weak ferromagnetic character of Fe. According to this character, due to the unfilled majority band, the Fe alloys are quite susceptible to internal or external perturbations. This is not the case of Fe–Cu alloys

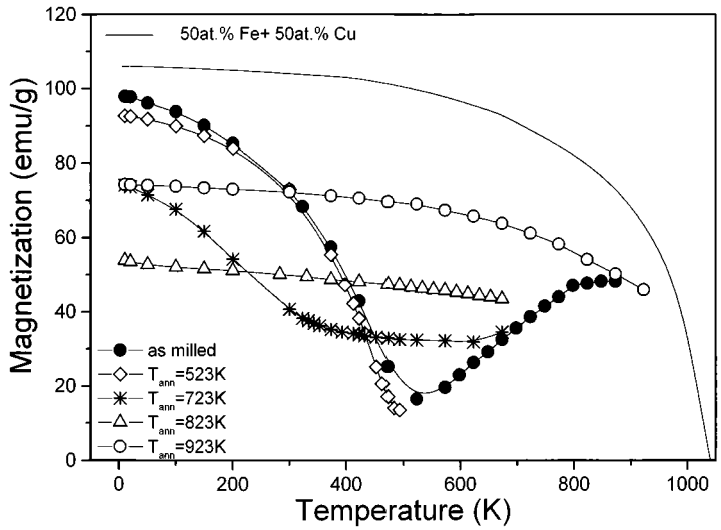

Figure 9. Thermal dependence of the magnetization for as-milled and heat treated $Fe_{50}Cu_{50}$ alloys measured under an applied field of $\mu_0 H = 1$ T. Solid line indicates the magnetization corresponding to an equiatomic mixture of bcc Fe and fcc Cu.

since the magnetic moment of the Fe atoms remains nearly constant up to very high Cu concentrations.

Hernando *et al* [52] studied the thermal dependence of the magnetization in as-milled and heat treated fcc $Fe_{50}Cu_{50}$. Their results indicated a magnetization deficit during thermal decomposition as is illustrated by figure 8. Since after decomposition bcc Fe and fcc Cu nanocrystals were well separated, the magnetization would be expected to increase or at least to remain with the same value as in the metastable fcc alloy. They attributed the magnetization deficit to the stabilization of the fcc Fe phase upon decomposition. The presence of the fcc Fe phase was proposed by Yavari [53] to be a consequence of a phase separation process via a spinoidal-like mechanism.

The nanocrystalline character of the alloy, combined with the peculiar separation mechanism, give rise to an unusual magnetization behaviour during the different steps of decomposition. Some of these striking features are briefly reported and discussed [54]. Figure 9 shows the temperature dependence of the magnetization for $Fe_{50}C_{50}$ alloy measured after heating at different temperatures. The most remarkable feature that can be observed in figure 9 is related to the evolution of the magnetization values at low temperature upon heating. In particular, after heating at 723 K the magnetization values had decreased by around 20% with respect to that of the as-milled material. Low temperature magnetic measurements pointed out that the thermal dependence of the magnetization does not follow the Bloch law but is linear. This behaviour can be explained as a consequence of a broad distribution of Curie temperatures [54]. Mössbauer analyses performed at room temperature in the as-milled alloy and after different heating treatments, as shown in figure 10, also indicate the presence of a complex mixing of different phases in the heated samples. After heating at 723 K the Mössbauer spectroscopy shows the presence of a paramagnetic phase at room temperature that should correspond with the remaining fcc Fe–Cu solid solution. This phase coexists with a high Curie temperature bcc phase attributed to the bcc Fe (Cu) also resolved by x-ray diffraction.

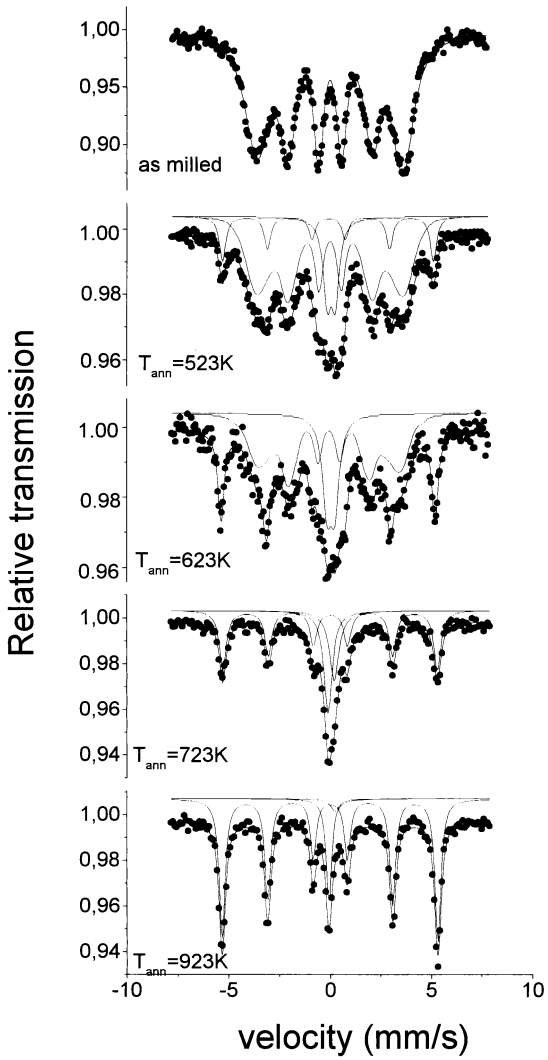

Figure 10. Room temperature Mössbauer spectroscopy of the fcc $Fe_{50}Cu_{50}$ alloy in the as-milled state and after heating at different temperatures.

4.3. Hints of a spinodal-like decomposition mechanism: broad distribution of Curie temperatures

The thermal dependence of coercivity also points out the coexistence of different phases intermixed at the nanoscale. Figures 11(a) and 11(b) illustrate both the dependence on temperature of the coercive field and the coercive field as a function of the annealing temperature, measured at 10 K and at room temperature, respectively. The soft magnetic behaviour of the as-milled solid solution is likely due to the negligible macroscopic anisotropy in the disordered alloy and to the nanocrystalline character of the sample. The coercive field of the as-milled sample decreases with temperature as is expected in any single-phase sample. Upon decomposition, the alloys exhibit the typical features of heterogeneous

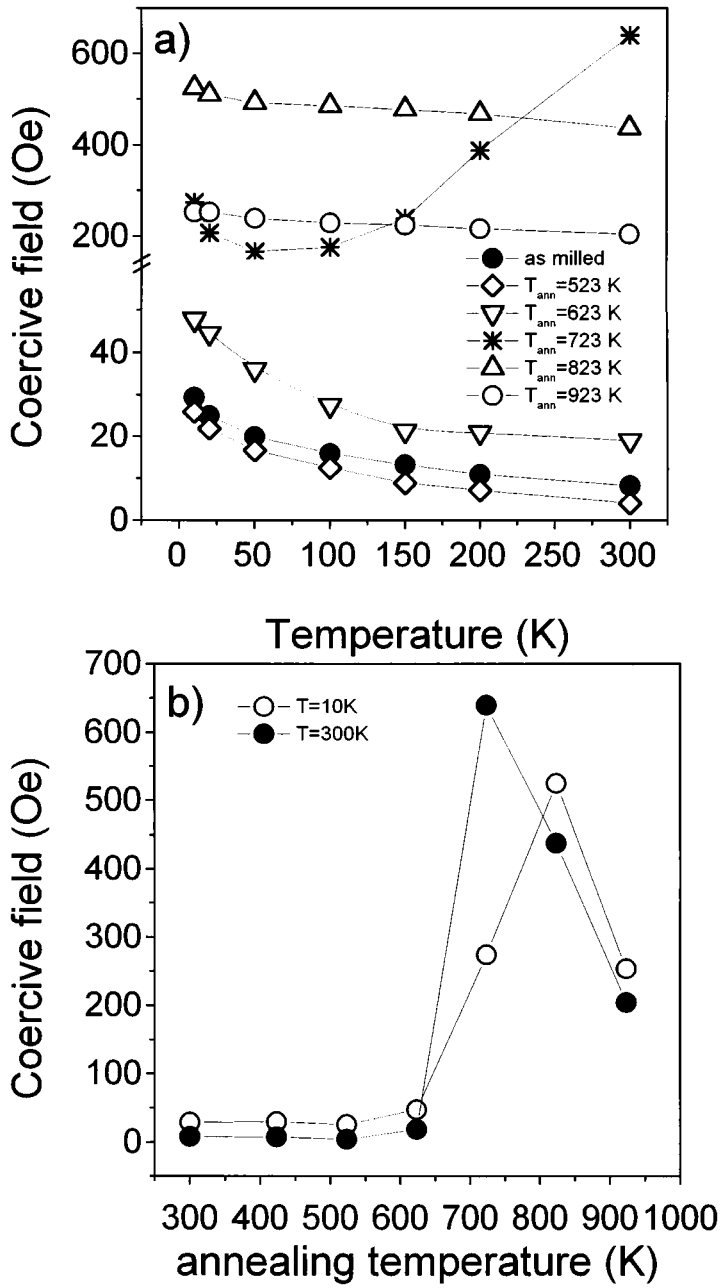

Figure 11. (a) Thermal dependence of the coercive field upon heating. (b) Dependence of the coercive field on the annealing temperature for the fcc $Fe_{50}Cu_{50}$ solid solution.

magnetic systems where phases with different Curie temperatures coexist. In such systems the thermal dependence of the coercive field depends, apart of the intrinsic properties, on the capability of the intergranular regions to transmit the exchange interactions between the randomly oriented grains. A detailed analysis of the thermal dependence of coercive

field in heterogeneous nanocrystalline systems has been recently reported by Hernando *et al* [55].

The coercive field of the $Fe_{50}Cu_{50}$ solid solution at room temperature depends on the heating temperature as shown in figure 11(b). The coercive field of the as-milled sample is 8 Oe at room temperature. This value does not appreciably change after annealing at temperatures below 723 K (except for a small increase probably associated with the appearance of bcc Fe phase as detected by Mössbauer). After heating at 723 K a remarkable increase of two orders of magnitude in coercive field is observed. The explanation of such a strong magnetic hardening can be found in the thermal dependence of the coercivity corresponding to this sample. According to x-ray data, the bcc Fe phase exhibits an average grain size of 20 nm. The grains are exchange isolated from other grains through the paramagnetic phase. The progressive isolation of bcc grains emerges from the increase of coercivity with temperature which can be clearly seen above 50 K. This anomalous thermal dependence of coercivity can only be explained as a consequence of the modifications of the degree of coupling between the ferromagnetic grains. Thus, the system behaves at room temperature as an assembly of single domains particles. The coercive field of 640 Oe corresponds to a typical value of coercivity for Fe single domains with spherical-like shape. It is important to note that the increase of coercivity takes place over a broad temperature range, from 50 to 300 K. This effect precludes the existence of a well defined Curie temperature of the phase separated bcc Fe grains, but unambiguously points out the existence of a distribution of exchange correlation lengths in the remaining fcc FeCu phase. This distribution of Curie temperatures can only be understood as a consequence of compositional fluctuations.

These experimental results cannot be understood by assuming that phase separation takes place via nucleation and grain growth of the stable phases. The broad distribution of Curie temperatures, detected from coercive force and magnetization measurements, seems to support the presence of a spinodal-like decomposition mechanism [53]. According to this type of decomposition, the composition profile along a particular direction, for instance x, can be described as $c(x) = c_0 + A\sin(kx)$ where c_0 is the initial composition, A the amplitude of the modulation and k the wave vector which generally corresponds to a wavelength of a few nanometres. The concentration waves develop along elastically soft directions giving rise to a lamellar structure. Some experimental evidence of a spinodal-like mechanism by TEM observations has been recently reported [55].

In conclusion, it has been well established that different steps of decomposition of immiscible alloys result in different nanostructures with strikingly different magnetic behaviour. Nanometric fluctuations of composition and symmetry lead to different ways to calculate weighted averages of the macroscopic properties, depending on the relative magnitude of the exchange coupling strength and the fluctuation length.

5. Thermal dependence of the effective anisotropy, Curie temperature enhancement and exchange coupling in two-phase nanostructures

Amorphous materials are sometimes considered as nanocrystals in the limit of zero crystal size. The 3d rich ferromagnetic amorphous alloys exhibit negligible macroscopic anisotropy due to the smoothing effect of the exchange. However, magnetostriction since it is a fourth rank tensor (as opposed to anisotropy), does not average out in random anisotropy systems. Therefore, residual stresses (always induced during the rapid quenching procedure) give rise to macroscopic anisotropy via magnetoelastic coupling, thus deteriorating softness. Softer amorphous materials are those, Co based, with low magnetostriction. Nevertheless, Co is a high

cost and restrictive magnetic element that prevents its use in high volume industrial production. That was the reason why the discovery of Fe rich soft nanocrystals carried out by Yoshizawa *et al* [56] in 1988 was really important. Typical compositions of the amorphous alloys which after partial devitrification reach nanostructures with optimal properties are FeSi and FeZr with small amounts of B to allow amorphization and much smaller amounts of Cu, which act as nucleation centres for crystallites, and Nb, which prevents grain growth. This effect is provided by Zr in FeZr alloys. After the first step of crystallization, FeSi or Fe crystallites are respectively finely dispersed in the amorphous matrix. In a wide range of crystallized volume fraction, the exchange correlation length of the matrix is larger than the average intergranular distance, d, and the exchange correlation length of the grains is larger than the grain size, D. Therefore, the smoothing effect of the exchange in a random anisotropy system drastically reduces the average structural anisotropy. Softness of Fe rich nanocrystals is also due to a second complementary reason: the opposite sign of the magnetostriction constant of crystallites and matrix which allows reduction and even compensation of the average magnetostriction [57].

Since the discovery of the soft nanocrystalline materials with great importance in technical magnetism, many scientific groups also realized the suitability of these systems to obtain more basic insight. Within a basic perspective, these systems are ideal to ask what is the appropriate weighted average of the macroscopic properties in two-phase systems strongly coupled by exchange through an enormous interface area. Classical articles on the basic aspects related to a nanoparticle system coupled at different degrees through a magnetic matrix start to appear in 1989: Herzer [58] gave a clear physical explanation to account for the softness of the nanocrystalline systems; Slawska-Waniewska *et al* [59] studied for the first time the superparamagnetic behaviour of the grains at temperatures above the Curie temperature of the matrix where the grain coupling is mainly magnetostatic. Hernando and Kulik [60], Slawska-Waniewska *et al* [61] and Grössinger *et al* [62] measured the thermal dependence of the coercivity for samples with different crystallized fraction and found multidomain, single-domain and superparamagnetic behaviour at different temperature ranges according to the strength of the intergranular coupling. Magnetic measurements in different compositions and under different conditions have also been continuously reported [63–72]. Thermally activated phenomena were analysed by Basso *et al* [73].

Based on the Herzer random anisotropy model of nanocrystals, Hernando *et al* [74] have developed a two-phase model which has been carefully analysed and improved by means of different measurements by Suzuki *et al* [75–77]. The summary of different results interpreted in the framework of the two-phase model has been recently published by Arcas *et al* [78]. Before going into a more detailed description of the effect of the interphase coupling on the magnetic properties, it must be mentioned that a parallel research effort has been carried out in the field of two-phase hard magnetic systems, also known as spring magnets. Since the discovery of the remanence enhancement by Davies' group [4] in NdFeB nanocrystalline systems embedded in a soft nanocrystalline Fe rich matrix, different studies have been oriented to understand the influence of coupling on the hardening and the enhancements of magnetic properties [79, 80]. The discovery of soft, Fe rich nanocrystals has given rise to an enormous interest in the crystallization details of these systems as well as in the nature of the intergranular region. Many articles dealing with detailed experimental observations on the crystallization process and its kinetics have been recently published [81–86].

Concerning the more intriguing and interesting experimental results caused by the existence of two phases mixed at nanoscale, let us, first, analyse the anomalous thermal dependence of the coercivity and, second, discuss (i) the possible existence of exchange coupling even above the Curie temperature of the matrix and (ii) the matrix Curie temperature enhancement due to exchange penetration from the grains with much higher Curie temperature.

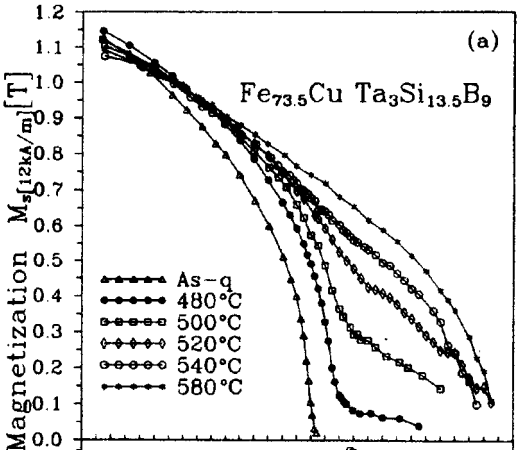

Figure 12. Temperature dependence of the magnetization $M_{s[12\ kA\ m^{-1}]}$ of the alloy studied in the as-quenched state and after one hour annealing at different temperatures.

5.1. Thermal dependence of temperature: exchange coupling above the Curie temperature of the matrix?

In [60] the thermal dependence of the coercivity has been studied in a system formed by α-Fe(Si) single-domain crystallites embedded in a soft amorphous matrix, whose Curie temperature, $T_{c[am]}$, is well below the Curie temperature of crystallites. Different volume fractions of crystallites, x, were obtained by annealing amorphous composition $Fe_{73.5}CuTa_3Si_{13.5}B_9$ at different temperatures (480, 500, 520, 540 and 580 °C) for 1 hour. Annealing at temperatures higher than 600 °C resulted in complete crystallization. From calorimetric measurements, the crystallized fraction x was estimated. According to x-ray diffractometry the average grain size, $D = 14$ nm, was roughly constant over the annealing temperature range. The intergranular average distance was estimated from D and x, according to the relation $d = D(1/x^{1/3}) - D$.

The temperature dependence of the magnetization shows behaviour typical for a material containing two ferromagnetic phases as shown in figure 12. From these curves an approximate value of $T_{c[am]}$ was obtained. The temperature dependence of the coercive field, illustrated by figure 13, exhibits a peak of coercivity in all the samples studied, which occurs at T_p. The intensity and the width of the peak strongly depend on the annealing temperature, as summarized in table 1. The curve describing the thermal dependence of the coercivity can be interpreted within the framework of the two-phase model [74, 78]. At room temperature the system is soft because the effective exchange between crystallites $A^* = \gamma(A_1A_2)^{1/2}$ is large enough to make the correlation length larger than both the intergrain distance, d, and the grain size. As the temperature rises and approaches $T_{c[am]}$, A_2 decreases and some grains start to be weakly coupled. The exchange correlation length decreases and the crystallites progressively start to act as pinning centres. Finally, when the temperature reaches $T_{c[am]}$ the grains form an assembly of exchange uncoupled single domains. Therefore the expected behaviour above $T_{c[am]}$ is that characteristic of a single domain presumably disturbed by dipole–dipole interactions. In some of the nanocrystalline samples the coercivity abruptly drops to zero above the peak temperature. Such a drastic decrease indicates a transition from a coupled two-phase system to a superparamagnetic regime. However, those samples with larger volume fraction exhibit a slow decrease above T_p.

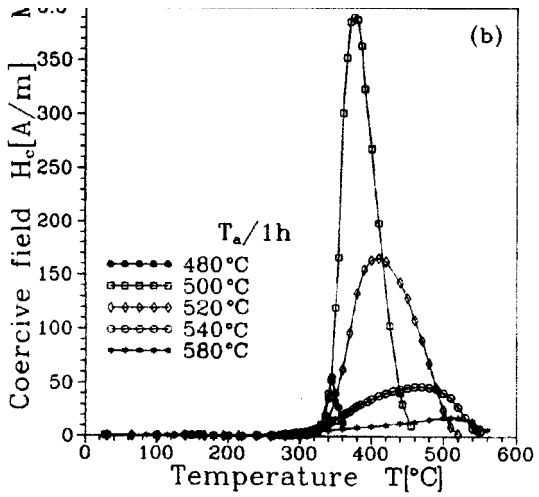

Figure 13. Thermal dependence of the coercive field H_c of the alloy studied in as-quenched state and after one hour annealing at different temperatures.

Table 1. Volume fraction of crystalline phase, X_1, Curie temperature $T_{c[am]}$ of amorphous phase and temperatures characterizing the peak of coercive field H_c of the alloy $Fe_{73.5}CuTa_3Si_{13.5}B_9$ in as-quenched state and after one hour annealing at different temperatures T_a (all temperatures are expressed in degrees centigrade).

T_a	X_1 (%)	$T_{c[am]}$	T_p
As-quenched	0	325	
480	15	358	345
500	43	367	375
520		380	410
540	69	326	470
580	75	296	510

T_p was expected to be located at $T_{c[am]}$ and that is the case for low annealing temperatures (480 and 500 °C). Nevertheless, for higher annealing temperatures T_p is shown to be well above $T_{c[am]}$. $(T_p - T_{c[am]})$ increases from 30 to 285 °C as the annealing temperature increases from 520 to 580 °C. This fact was interpreted [60] as evidence that the exchange coupling between the grains takes place even above the Curie temperature of the matrix when they are close enough. Notice that the average intergranular distance for annealing temperatures of 520 and 580 °C ranges from 4 nm to 1 nm. Nevertheless, it should be indicated that Herzer [3] has shown later that dipole–dipole interactions derived from the blocking temperature could also account for the difference between T_p and $T_{c[am]}$.

5.2. Does the exchange field of grains penetrate into the matrix?

An interesting question related to the coupling between two phases with large interface area is the mutual influence on the values of their Curie temperatures. Experiments carried out on this subject in either thin layers or granular nanocrystals have been shown to be non-conclusive. The reason is the lack of a deep knowledge about the nature of the interface. Unavoidable mixing of atoms at the interface gives rise to the formation of thin layers of alloys with unknown composition and therefore unknown Curie temperatures. But with great generality it can be

said that the gradient of properties at the interfaces induces drastic changes in the expected Curie temperature of nanometric phases. Let us show some experimental results obtained in nanocrystals of Fe [87]. Starting from the amorphous composition $Fe_{77}B_{18}Nb_{5.1}Cu_{1.3}$, after annealing in the temperature range from 455 to 700 °C, samples were obtained formed of bcc α-Fe nanocrystals, with crystallized fractions $x = 8$, 14, 22, 28, 32 and 39 at.%, embedded in an amorphous matrix. The volume fraction was estimated from the relative resonant area of the Mössbauer spectra and the grain size from x-ray diffraction pattern through Scherrer formula. The composition of the amorphous matrix, different for different annealing temperature, was obtained from the crystallized fraction, x. Amorphous ribbons with the same composition that the amorphous matrix were also rapidly quenched in order to compare their Curie temperatures.

Table 2 shows the estimated amorphous interphase composition and relevant parameters. $T^*_{c[am]}$ corresponds to the Curie temperature of the composition as cast by melt spinning and $T_{c[am]}$ is the Curie temperature of the composition when the matrix is Fe nanocrystals.

Table 2. Crystallized volume fraction, X_1 estimated matrix composition, grain size D, intergrain distance, d, Curie temperature of the matrix and Curie temperature of the same amorphous composition free of Fe crystallites in $Fe_{77}B_{18}Nb_4Cu$ alloy, in the as-cast and in nanocrystalline samples annealed at different temperatures.

T_{ann} (°C)	X_1	Estimated amorphous matrix composition	D (nm)	d (nm)	T_c^a (°C)	T_c^{a*} (°C)
As cast	0	$Fe_{77}B_{18}Nb_4Cu$			214	214
455	8	$Fe_{75.5}B_{19.2}Nb_{4.3}Cu$	9	12	273	220
475	14	$Fe_{74.2}B_{20.2}Nb_{4.5}Cu_{1.1}$	10	11	298	225
510	22	$Fe_{73.5}B_{20.7}Nb_{4.5}Cu_{1.2}$	10	7	343	235
530	28	$Fe_{70.7}B_{22.9}Nb_{5.1}Cu_{1.3}$	10	5	355	240
555	32	$Fe_{69.5}B_{23.9}Nb_{5.3}Cu_{1.3}$	10	4	365	235
580	32	$Fe_{69.5}B_{23.9}Nb_{5.3}Cu_{1.3}$	11	4	364	235
590	39	$Fe_{67.1}B_{25.7}Nb_{5.7}Cu_{1.4}$	12	4	355	230

The difference $T_{c[am]} - T^*_{c[am]}$ increases up to 95 °C as the average distance between Fe crystallites decreases to 4 nm. From the magnetic point of view there are two possible types of interaction which could be invoked to account for this phenomenon: (i) exchange field penetration and/or (ii) magnetostatic field polarizing the matrix above its Curie temperature, at which the susceptibility diverges, giving rise to an apparent increase of the order temperature. The difference between these interactions is in their ranges. The magnetostatic interaction is long range and can take a maximum value of 2 T in the whole volume of the matrix. On the other hand, the effective molecular field within α-Fe particles is close to 1000 T, but is expected to decay exponentially in one or two atomic distances along the perpendicular direction to the interface and inwards toward the matrix. Therefore, if we consider the exchange penetration to be restricted to an interatomic distance at which the molecular field is 500 T, the matrix thickness for which both magnetostatic and exchange field takes the same volume average should correspond to 500 interatomic distances. For shorter matrix thickness the exchange field, even decreasing so rapidly, becomes much larger than the magnetostatic one. This argument is quite relevant in nanostructured magnetic systems, for which exchange interactions becomes stronger than magnetostatic ones. As the increase in Curie temperature due to the Fe crystallites reaches a value of 100 °C corresponding to 80 T the only interaction with strength high enough to account for this effective field is the exchange.

As stated above there is another, non-magnetic, possible cause that could be invoked to account for the difference $T_{c[am]} - T^*_{c[am]}$. This cause has been proposed by Yavari [84] and can be explained in terms of diffusion layers and sharp concentration gradients. The

difference in diffusion rates between Nb and B, both rejected toward the matrix area during crystallization, results in a flat profile of B concentration throughout the matrix thickness but a sharp concentration of Nb around the Fe crystallite surface. The Curie temperature of the matrix should be that of the large volume Nb poor–B rich region with higher Curie temperature than that of an amorphous alloy corresponding to the global composition. Estimation of the possible $T_{c[am]} - T^*_{c[am]}$ expected from experimental results performed with different Nb and B contents indicates that 25 °C should be the maximum difference due to compositional gradients. It can be summarized that exchange penetration is likely the main cause of the Curie temperature enhancement of the matrix, but one cannot discard contributions from magnetostatic interaction as well as compositional sharp gradients.

Even though different observations performed in multilayers and spring magnets also support the plausibility of the exchange field penetration assumption, an open field remains to be explored with high resolution experimental techniques.

6. Conclusions

It can be concluded that the studies in magnetism of nanocrystalline systems have been strongly stimulated by the development of non-equilibrium fabrication techniques, high resolution experimental methods and surprisingly outstanding macroscopic magnetic properties. Nanostructured systems become ideal samples for analysis of basic aspects such as interface magnetism, interactions and influence of nanoscale fluctuations of the local magnetic properties on the macroscopic behaviour. Nanocrystalline samples are nowadays used in the classical magnetic technology as hard and soft magnetic materials. These type of material are also promising candidates for increasing the memory density in magnetic storage and recording. An interesting field of research is still open in order to understand magnetic relaxation and the intimate coupling between core and shell in particles isolated magnetically as well as between crystallite and grain boundaries.

Acknowledgments

The author is indebted to Dr J M Rojo for inspiration, moral support and his contributions to understanding some aspects of this work.

He also thanks Dr J Torrance, Dr C Ortiz, Dr A Berkowitz, Dr G Hadjipanayis, Dr M Vázquez, Dr J M González, Dr P Crespo, Dr P Marín and Dr A González for helpful discussions and C Jurado and A Morala for valuable help in the editing.

References

[1] Xiao J Q, Jiang J S and Chien C L 1992 *Phys. Rev. Lett.* **68** 3749
Berkowitz A E, Mitchell J R, Carey M J, Young A P, Zhang S, Spada F E, Parker F T, Hutten A and Thomas G 1992 *Phys. Rev. Lett.* **68** 3745
[2] Chien C L, Liou S H, Kofalt D, Yu Wu, Egami T and McGuire T R 1986 *Phys. Rev.* B **33** 3247
Mazzone G and Vittori Antisari M 1996 *Phys. Rev.* B **54** 441
[3] Herzer G 1995 *Scr. Metall. Mater.* **33** 1741
[4] Kronmüller H, Fischer R, Seeger M and Zern A 1996 *J. Phys. D: Appl. Phys.* **29** 2274
Manaf A, Buckley R A, Davies H A and Leonowicz M 1991 *J. Magn. Magn. Mater.* **101** 360
[5] It is not possible to increase substantially either the number of atoms per unit volume or the atomic magnetic moment.
[6] Bertotti G 1998 *Hysteresis in Magnetism* (London: Academic) p 170
[7] Alben R, Becker J J and Chi M C 1978 *J. Appl. Phys.* **49** 1653

Herzer G 1989 *IEEE Trans. Magn.* **25** 3327

[8] Related to relaxation and magnetization reversal see for instance the following books and articles:
Hadjipanayis G C and Prinz G (eds) 1991 *Science and Technology of Nanostructured Magnetic Material (NATO ASI Series B; Physics 259)*
Hadjipanayis G and Siegel R W (eds) 1994 *Nanophase Materials (NATO ASI Series E: Applied Sciences 260)*
Hernando A (ed) 1993 *Nanomagnetism (NATO ASI Series E: Applied Sciences 247)*
Dormann J L, Fiorani D and Tronc E 1997 *Advances in Chemical Physics XCVIII* eds I Prigogine and S A Rice ISBN 0-471-16285-X (New York: Wiley) pp 283–493
Labarta A, Iglesias O, Balcells Ll and Badía F 1993 *Phys. Rev.* B **48** 10 240
Lederman M, Schultz S and Ozaki M 1994 *Phys. Rev. Lett.* **73** 1986
González J M, Ramirez R, Smirnov-Rueda R and González J 1995 *Phys. Rev.* B **52** 16 034
García del Muro M, Batlle X, Labarta A, González J M and Montero M I 1997 *J. Appl. Phys.* **81** 7427
Martínez-Albertos L, Miranda R and Hernando A 1997 *Phys. Rev.* B **55** 11 080
López-Quintela M A and Rivas J 1993 *J. Colloid Interface Sci.* **158** 446
Other new and interesting systems are those formed by magnetic particles distributed in a superconducting matrix, see, for instance,
Martin J I, Jaccard Y, Hoffmann A, Nogués J, George J M, Vicent J L and Schuller I K 1998 *J. Appl. Phys.* **84** 411
Jaccard Y, Martin J I, Cyrille M C, Vélez M, Vicent J L and Schuller I K 1998 *Phys. Rev.* B **58** 8232

[9] Morup S, Bodker F, Hendriksen P V and Linderoth S 1995 *Phys. Rev.* B **22** 287

[10] Shtrikman S and Wohlfarth E P 1981 *Phys. Rev. Lett.* A **85** 467

[11] Dormann J L, Bessasis L and Fiorani D 1988 *J. Phys. C: Solid State Phys.* **21** 2015

[12] Chudnovsky M and Tejada J 1998 *Quantum Tunneling of the Magnetic Moment* (Cambride: Cambridge University Press)

[13] Gleiter H 1990 *Prog. Mater. Sci.* **33** 223
Fultz B, Kuwano H and Ouyang H 1995 *J. Appl. Phys.* **77** 3458

[14] Del Bianco L, Hernando A, Bonetti E and Navarro E 1997 *Phys. Rev.* B **56** 8894
del Bianco L, Ballesteros C, Rojo J M and Hernando A 1998 *Phys. Rev. Lett.* **81** 4500

[15] Morrish A H, Haneda K and Zhou Z X 1994 *Nanophase Materials (NATO ASI Series E: Applied Sciences. 260)* eds G C Hadjipanayis and R W Siegel (Dordrecht: Kluwer) pp 515–35

[16] Hanson M and Nilsson B 1994 *Nanophase Materials (NATO ASI Series E: Applied Sciences 260)* ed G C Hadjipanayis and R W Siegel (Dordrecht: Kluwer) p 569

[17] Morup S and Linderoth S 1994 *Nanophase Materials (NATO ASI Series E: Applied Sciences. 260)* ed G C Hadjipanayis and R W Siegel (Dordrecht: Kluwer) p 595

[18] Vincent P, Hammann J, Prené P and Tronc E 1994 *J. Physique* I **4** 273

[19] Morup S and Tronc E 1994 *Phys. Rev. Lett.* **70** 3278

[20] Awschalom D D, Smyth J F, Grinstein G, DiVincenzo D P and Loss D 1992 *Phys. Rev. Lett.* **68** 3092

[21] Kodama R H, Berkowitz A E, McNiff E J and Foner S 1996 *Phys. Rev. Lett.* **77** 394

[22] Berkowitz A E, Spada F E and Parker F T 1994 *Nanophase Materials (NATO ASI Series E: Applied Sciences 260)* ed G C Hadjipanayis and R W Siegel (Dordrecht: Kluwer) p 587

[23] Kodama R H, Berkowitz A E, McNiff E J Jr and S Foner 1997 *J. Appl. Phys.* **81** 5552

[24] Martínez B, Obradors X, Balcells Ll, Rouanet A and Monty C 1998 *Phys. Rev. Lett.* **80** 181
del Bianco L, Hernando A, Multigner M, Prados C, Sánchez López J C, Fernández A, Conde C F and Conde A 1998 *J. Appl. Phys.* **84** 2189

[25] Gangopadhyay S, Hadjipanayis C G, Sorensen C M and Klabunde K J 1994 *Nanophase Materials (NATO ASI Series E: Applied Sciences 260)* eds G C Hadjipanayis and R W Siegel (Dordrecht: Kluwer) p 573

[26] Sun S W and O'Handley R C 1991 *Phys. Rev. Lett.* **66** 2798

[27] Hernando A, Navarro E, Multigner M, Yavari A R, Fiorani D, Rosenberg M, Filoti G and Caciuffo R 1998 *Phys. Rev.* B **58** 5181

[28] Hernando A, Rojo J M, Yavari R, Navarro E, Barandiarán J M and Ibarra M R 1997 *Mater. Sci. Forum* **235–238** 675
Shirane G, Chen C W and Flinn P A 1963 *Phys. Rev.* **131** 183

[29] Kouvel J S 1966 *J. Appl. Phys.* **37** 1257

[30] Ibarra M R and Algarabel P A 1994 *Phys. Rev.* B **50** 4196

[31] Moruzzi V L and Marcus P M 1992 *Phys. Rev.* B **46** 2864

[32] Hernando A, Navarro I, Prados C, García D, Vázquez M and Alonso J 1996 *Phys. Rev.* B **53** 13 8223

[33] May F, Srivastasa P, Farle M, Bovensiepen U, Wende H, Chauvistre R and Barbeschke K 1998 *J. Magn. Magn. Mater.* **177–181** 1220

[34] Gonzalez E M, Montero M I, Cebollada F, de Julian C, Vicent J L and Gonzalez J M 1998 *Europhys. Lett.* **42** 91
[35] Lewis L H, Welch D O and Panchanathan V 1997 *J. Magn. Magn. Mater.* **175** 275
[36] Hernando A, González A, Ballesteros C, Zern A, Fiorani D, Lucari F and D'Orazio F 1999 *IWOMP (Bolonia, 1999) Nanostruct. Mater.* at press
[37] Slawska-Waniewska A and Greneche J M 1997 *Phys. Rev.* B **56** R8491
Orúe I, Gorría P, Plazaola M L, Fernández-Gubieda M L and Barandiarán J M 1994 *Hyperfine Interact.* **94** 2199
[38] Liu T, Gao Y F, Zu Z X, Zhao T and Ma R Z 1996 *J. Appl. Phys.* **80** 3972
Kemény T, Varga L K, Kiss L F, Balogh J, Lovas A, Toth T and Vincze L *9th Int. Conf. on Rapidly Quenched and Metastable Materials* (Elsevier) suppl p 201
[39] Randrianantoandro N, Slawska-Waniewska A and Greneche J M 1997 *Phys. Rev.* B **56** 10 797
[40] Coey J M D 1971 *Phys. Rev. Lett.* **27** 1140
Berkowitz A E, Lahut J A and VanBuren C E 1980 *IEE Trans. Magn.* **16** 184
[41] Baibich M N, Broto J M, Fert A, Nguyen van Dau F, Petroff F, Etienne P E, Creuzet G, Friedich A and Chazelas J 1998 *Phys. Rev. Lett.* **61** 2472
[42] Allia P, Knobel M, Tiberto P and Vinai F 1995 *Phys. Rev.* B **52** 15 398
Madurga V, Ortega R J, Vergara J, Elvira R, Korenivski V and Rao K V 1995 *Mater. Res. Soc. Proc. Symp.* vol 384 (Pittsburgh, PA: Materials Research Society) p 541
Ribbons of FeCu alloys have been also produced:
Gómez Polo C, Hernando A and El Ghanami M 1998 *J. Magn. Magn. Mater.* **187** 117 and references therein
[43] Sumiyama K, Yoshitake T and Nakamura Y 1984 *J. Phys. Soc. Japan* **53** 3160
[44] Chien C L, Liou S H, Kofalt D, Yu Wu, Egami T and McGuire T R 1984 *Phys. Rev.* B **33** 3160
[45] Jilman P S and Benjamin J S 1983 *Annu. Rev. Mater. Sci.* **13** 279
[46] Uenishi K, Kobayashi K F, Nasu S, Hatano H, Ishishara K N and Shingu P U 1992 *Z. Metallkd.* **83** 32
Shingu P H, Ishiara K N, Uenishi K, Kuyama J, Huang B and Nasu S 1990 *Solid State Powder Proc.* ed A H Claver and J J de Barbadillo (Minerals, Metals and Materials Society) p 21
[47] Ma E, Atzmon M and Pinkerton F E 1993 *J. Appl. Phys.* **74** 955
[48] Eckert J, Birrinerg R, Holzer J C, Krill C E and Johnson W L 1992 *Proc. Mater. Res. Soc. Symp.* vol 238 (Pittsburgh, PA: Materials Research Society) p 739
[49] Eckert J, Holzer J C, Krill C E and Johnson W L 1993 *J. Appl. Phys.* **73** 2794
[50] Yavari A R, Desré P J and Benameur T 1992 *Phys. Rev. Lett.* **68** 2235
[51] Harris V G, Kemmer K M, Das B N, Koon N C, Ehrlich A E, Kirkland J P, Woicik J C, Crespo P, Hernando A and García-Escorial A 1996 *Phys. Rev.* B **54** 6929
[52] Hernando A, Crespo P, García Escorial A and Barandiarán J M 1993 *Phys. Rev. Lett.* **70** 3521
[53] Yavari A R 1993 *Phys. Rev. Lett.* **70** 3522
[54] Crespo P, Hernando A, Yavari R, Drbohlav O, García Escorial A, Barandirán J M and Orué I 1993 *Phys. Rev.* B **48** 7134
Crespo P, Hernando A and García Escorial A 1994 *Phys. Rev.* B **49** 13 227
[55] Hernando A, Crespo P, García Escorial A, Barandiarán J M, Urchulutegui M and Vittori Antisari M 1995 *Europhys. Lett.* **32** 585
[56] Yoshizawa Y, Oguma S and Yamauchi K 1988 *J. Appl. Phys.* **64** 6044
[57] Herzer G 1990 *IEEE Trans. Magn.* **26** 1397
[58] Herzer G 1996 *J. Magn. Magn. Mater.* **157/158** 133
[59] Slawska-Waniewska A, Gutowski M, Lachowicz H, Kulik T and Matyja H 1992 *Phys. Rev.* B **46** 14 594
[60] Hernando A and Kulik T 1994 *Phys. Rev.* B **49** 7064
[61] Slawska-Waniewska A, Nowicki P, Lachowicz H K, Gorría P, Barandiarán J M and Hernando A 1994 *Phys. Rev.* B **50** 6465
[62] Grössinger R, Holzer D, Kussbach C, Sassik H, Sato-Turtelli R, Sinnecker J P and Wittig E 1995 *IEEE Trans. Magn.* **31** 3883
[63] Vo Hong Duong, Grössinger R, Sato Turtelli R and Polak Ch 1996 *J. Magn. Magn. Mater.* **157/158** 193
[64] Caro P, Cebollada A, Briones F and Toney M F 1998 *J. Cryst. Growth* **187** 426
Caro P, Cebollada A, Ravelosona D, Tamayo J, Garcia R and Briones F 1998 *Acta Mater.* **46** 2299
Konc M, Kovác J, Dusa O, Svec T and Sovak P 1995 *J. Magn. Magn. Mater.* **146** 17
[65] Vázquez M, Marín P, Davies H A and Olonfijana A O 1994 *Appl. Phys. Lett.* **64** 3184
Vázquez M and Zhukov A P 1996 *J. Magn. Magn. Mater.* **160** 223
[66] Lachowicz H K 1995 *J. Korean Magn. Soc.* **5** 589
[67] Hogsdon S N, Squire P T, del Real R P and Kulik T 1995 *IEEE Trans. Magn.* **31** 3895
[68] Gorría P, Orué I, Fernández-Gubieda M L, Plazaola F, Zabala N and Barandiarán J M 1996 *J. Magn. Magn. Mater.* **157/158** 203

[69] Varga L K, Kisdi-Koszó É, Ström V and Rao K V 1996 *J. Magn. Magn. Mater.* **159** L321
[70] Yu Xiaojun, Quan Baiyun, Sun Guigin and Narita Kenji 1995 *J. Korean Magn. Soc.* **5** 507
[71] Orúe I, Fndez-Gubieda M L, Plazaola F and Barandiarán J M 1998 *J. Phys.: Condens. Matter* **10** 3807
Bordin G, Buttino G, Cecchetti A and Poppi M 1995 *J. Magn. Magn. Mater.* **150** 363
[72] Ravach G, Teillet J, Fnidiki A, Le Breton J M, Driouch L and Hassanain N 1996 *J. Magn. Magn. Mater.* **157/158** 173–74.
[73] Basso V, LoBue M, Beatrice C, Tiberto P and Bertoti G 1998 *IEEE Trans Magn.* **34** 1177
[74] Hernando A, Vázquez M, Kulik T and Prados C 1995 *Phys. Rev.* B **51** 3581
[75] Suzuki K and Cadogan J M 1998 *Phil. Mag. Lett.* **77** 371
[76] Suzuki K and Cadogan J M 1998 *Phys. Rev.* B **58** 2730
[77] Suzuki K, Makino A, Inoue A and Masumoto T 1993 *J. Appl. Phys.* **74** 3316
[78] Arcas J, Hernando A, Barandiarán J M, Prados C, Vázquez M, Marín P and Neuweiler A 1998 *Phys. Rev.* B **58** 5193
[79] Fischer R and Kronmuller H 1996 *Phys. Rev.* B **54** 7284
[80] Fischer R, Schrefl T, Kronmuller H and Fidler J 1996 *J. Magn. Magn. Mater.* **153** 35
[81] Greer A L 1985 *Rapidly Quenched Metals* ed S Steeb and H Warlimont (Elsevier) p 215
[82] Muller M, Mattern N and Illgen I 1991 *Z. Metallkde* **82** 895
[83] Conde C F, Millán M, Borrego J M, Conde A, Capitán M J and Joulaud J L 1998 *Phil. Mag. Lett.* **78** 221
[84] Yavari A R 1997 *Mater. Sci. Eng.* A **226/228** 491
[85] Fernández-Barquín L, Gómez Sal J C, Gorría P, Gariotaonandia J S and Barandiarán J M 1998 *J. Phys.: Condens. Matter* **10** 5027
Barandiarán J M, Gorría P, Orue I, Fernández Gubieda M L, Plazaola F, Gómez Sal J C, Fernández Barquín L and Fournes L 1977 *J. Phys.: Condens. Matter* **9** 5671
Gorría P, Garitaonandia J S and Barandiarán J M 1996 *J. Phys.: Condens. Matter* **8** 5925
Cebollada F, González J M, De Julián C and Suriñach S 1997 *Phys. Rev.* B **56** 6056
[86] Clavaguera-Mora M T, Baró M D, Suriñach S and Clavaguera N 1990 *J. Mater. Res.* **5** 1201
[87] Hernando A, Navarro I and Gorría P 1995 *Phys. Rev.* B **51** 3281